JOURNAL OF THE CIVIL ENGINEERING FORUM

Journal of the Civil Engineering Forum, May 2021, 7(2): 223-238
DOI 10.22146/jcef.62930
Available Online at HTTP: https://jurnal.ugm.ac.id/jcef/issue/archive

Behaviour of Precast Concrete Beam-to-Column Connection with SHS Hidden Corbel Subjected to Monotonic Load

Jen Hua Ling[1,*], Jee Hock Lim[2], Ahmad Baharuddin Abd. Rahman [3]
[1] School of Engineering and Technology, University College of Technology Sarawak, Sarawak, MALAYSIA
96000 Sibu, Sarawak, Malaysia
[2] Department of Civil Engineering, Universiti Tunku Abdul Rahman, Selangor, MALAYSIA
43000 Selangor, Malaysia
[3] Department of Structures and Materials, School of Civil Engineering, Universiti Teknologi Malaysia, Johor, MALAYSIA
81310 Skudai, Johor Darul Ta'zim, Malaysia
*Corresponding authors: lingjenhua@ucts.edu.my

SUBMITTED 7 January 2021 **REVISED** 29 January 2021 **ACCEPTED** 4 February 2021

ABSTRACT Beam-to-column connection is the most critical part of a precast concrete (PC) that governs the integrity of the entire structure, hence its characteristics need to be determined for safe applications in the construction industry. Therefore, this study developed a beam-to-column connection with square hollow section (SHS) hidden corbel. A full-scale test was conducted on eleven T-subframe specimens with various configurations used to investigate the behaviour of the connection under an incremental static load. It was further evaluated using the beam-line method to determine the moment-rotation response and the mechanical properties. Furthermore, this research analyzed the parametric response, the load resisting mechanism, and the feasibility of the connection for PC structures. Due to extensive usage of steel elements, the PC connection gave a higher ultimate strength than the reinforced concrete (RC). Its moment resistance was largely contributed by the hidden corbel embedded in the beam and column, increasing with the column and beam's embedded length. The grout infill prevented the lateral deformation of the hidden corbel and hence strengthened the connection. Due to the low bending resistance of the steel endplate, the PC connection possessed a low stiffness, which led to a larger rotation deformation than the RC connection, and a low design strength. This could be overcome by modifying the shape of the endplate for a higher second moment of inertia in resisting bending. The PC connection was classified as semi-rigid and partial-strength, and only specimen PC-3 was considered feasible for PC structures.

KEYWORDS Beam-to-column connection; Precast; Hidden corbel; Beam-line method; Full-scale test.

1 INTRODUCTION

Precast concrete (PC) is one of the construction methods popularly used in Malaysia. The building elements are prefabricated in factories under controlled environments with good quality assurance before being transported to construction sites for installation. This permits the rapid erection of PC structures with less energy and labour consumption, including low risk of occupational safety and health (Zheng et al., 2018; Lu et al., 2019; Lin & Zhao, 2020).

The joint between the building elements is normally the weakest part of a PC structure (Choi et al., 2013). It governs the behaviour and integrity of the entire structure. The beam-to-column connection in PC is a joint between a beam and a column. It is designed to have the ability to transfer loads from a member to another, such as shear, moment, axial, torsion, etc. The connection needs to be reliable, for structural stability, and preferably easy-to-install for speedy construction.

However, the connections for a wide variety of designs possess unique characteristics. Therefore, it is important to realize the behaviour of a connection for this purpose. Although PC elements are made of concrete, the connections demonstrate the characteristics of steel joints. This is due to the extensive use of steel components to transfer loads and facilitate installations.

For the low deformability of concrete, the PC connection normally fails with excessive cracks before the failure of the steel elements. Hence, determining the properties of the connection solely based on the steel components is likely overestimating its performance. Therefore, the beam-line method is used to determine the properties of a PC connection (Elliott, 2002). These are further used to classify the connection in respect to the Eurocode 3 (BS EN 1993-1-8:2005).

The characteristics of a newly developed beam-to-column connection can be determined using the full-scale destructive test (Jaspart, 1996; Lim, 2014). In this study, a beam-to-column connection with a hidden corbel made of square hollow section (SHS) was developed for non-seismic applications. An experimental test was carried out to acquire the structural behaviour as well as classify the connection. The parametric response and the load resisting mechanism of the connection were also analyzed. Furthermore, the feasibility of the connection in PC structures was evaluated.

2 METHODS

2.1 Specimen Details

Eleven full-scale T-subframe specimens were fabricated and tested under incremental monotonic load. This included 2 control (i.e. RC0 and PC0) and 9 test specimens (i.e. PC1 to PC9), each of which comprised of a square column and rectangular beam, designed with respect to the common sizes and reinforcements used in the local construction industry (Figure 1 and Table 1). The load was applied on the beam at a distance of 1375 mm from the column face.

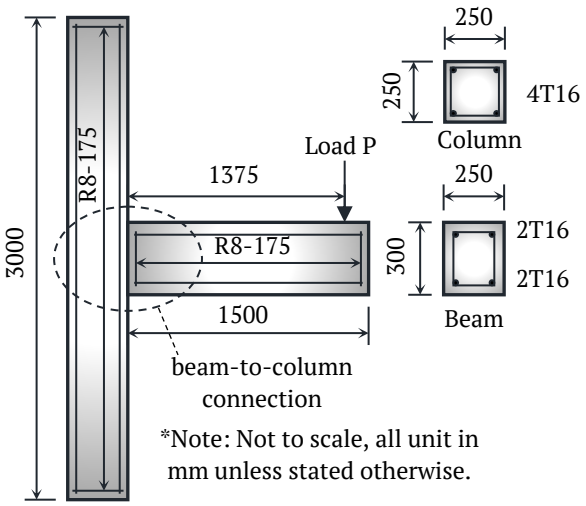

Figure 1. Details of specimen

The configuration of the specimens are described as follows

a) Specimen RC0 represented a reinforced concrete (RC) joint (Figure 2(a)). The concrete was monolithically cast without a cold joint (Figure 3). The steel bars of the beam were embedded in the column at full anchorage length.
b) Specimen PC0 resembled a PC connection without an SHS hidden corbel (Figure 2(b)). The steel bars in the beam were welded on a 20 mm thick steel endplate of grade S275. In addition, the endplate was further bolted to the column.
c) Specimens PC1 to PC9 were PC connections with SHS hidden corbels (Figure 2(c)). The design was identical to PC0 except for the 2 SHSs of different sizes embedded in the beam. Meanwhile, during installation, the smaller SHS was slid and inserted into the column before the grout was poured into the void (Figure 4).

Table 1. Dimension of specimen

	Beam	Column
Dimension	250 mm x 300 mm x 1500 mm	250 mm x 250 mm x 3000 mm
Reinforcements	Top and bottom bars, high yield strength steel bars 2T16 (f_{sy} = 460 N/mm^2)	High yield strength steel bars, 4T16 (f_{sy} = 460 N/mm^2)
Shear links	Mild steel bars, R8-175 (f_{sy} = 250 N/mm^2)	Mild steel bars, R8-175 (f_{sy} = 250 N/mm^2)
Concrete cover	41 mm	25 mm

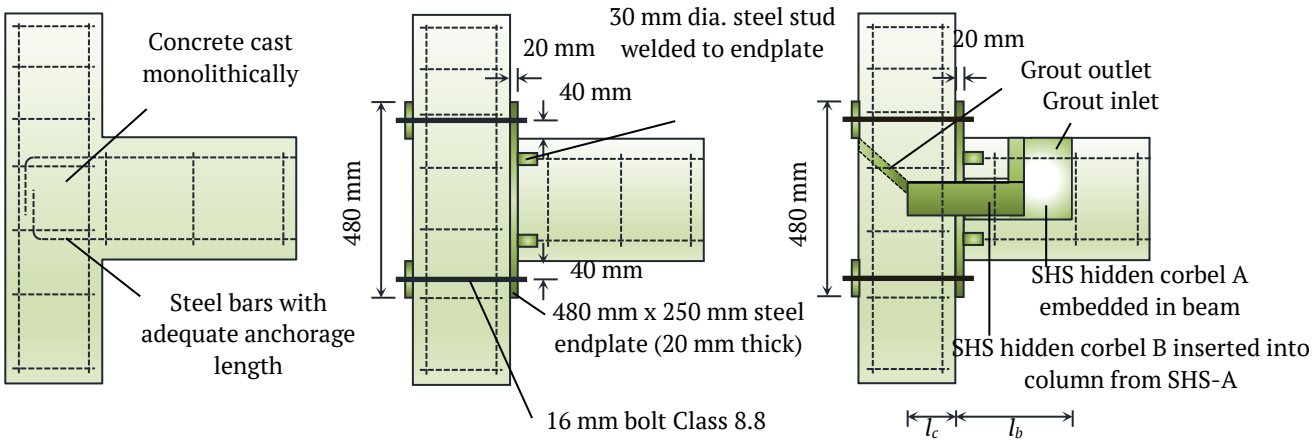

(a) RC0 (Control) (b) PC0 (Control) (c) PC1-9

Figure 2. Design of specimens

(a) Reinforcement and formworks (b) Monolithic casting

Figure 3. Preparation of specimen RC0

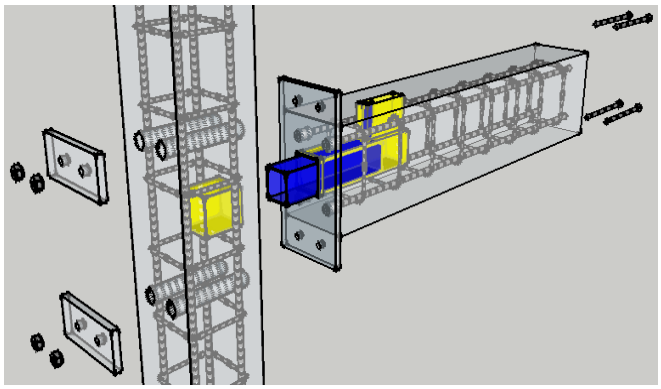

Figure 4. Installation of the connection

The details of the connections are shown in Table 2. The parameters studied included

a) Effects of PC beam-to-column connection (RC0 vs PC0-9)
b) Effects of SHS hidden corbel (PC0 vs PC1-9)
c) Effects of the hidden corbel size (PC1-3)
d) Effects of the embedded length of hidden corbel in column (PC3-5)
e) Effects of the embedded length of hidden corbel in beam (PC3, 6, and 7)
f) Effects of grout in hidden corbel (PC3, 8, and 9)

The specimens were horizontally cast with grade 40 ready-mixed concrete in the laboratory. The design slump was relatively 50 mm to 100 mm while the maximum aggregate size was 20 mm. The specimens were cured under moisture with wet jute sacks for 7 days before installation on the 28th day.

Subsequently, high strength and non-shrink grout (Brand: *Sika-215*) of grade 70 was mixed into a pourable state during installation. The proportion of the mixture comprised 4 litres of water per 25 kg of grout power. The grout was poured into the hidden corbel through its inlet until an overflow was detected at the outlet. The compressive strength of the grout was closely monitored until that which was intended was achieved before the specimens were tested.

2.2 Test Setup

Steel frames were assembled in the laboratory to test the specimens. The support frame held the column in position while the load frame induced vertical load onto the beam (Figures 5(a) and (b)). The column was restrained from horizontal displacement and moment rotation by inserting its ends in the grip buckets.

A hydraulic cylinder (Brand: *Enerpac*, capacity: 250 kN) was used to generate the load acting on the beam at a distance of 1375 mm from the column face. A load cell (Brand: *TML*, capacity: 100 kN) was used to measure the weight on the beam. In addition, twelve linear variable displacement transducers (LVDT) (Brand: *TML*) and 2 inclinometers (Brand: *AccuStar*) were used to measure the displacement and rotation of the column and beam of the specimens (Figure 5(c)). Furthermore, six LVDTs (H_1 to H_6) were used to measure the horizontal displacement of the column. Meanwhile, another six (V_1 to V_6) were used to determine the vertical displacement of the beam. All the measuring devices were connected to a logger (Brand: *TML*, 30 channels) for data acquisition.

Once the setup was completed, all readings were initialized to zero. The load was progressively increased at a rate of approximately 2.5 kN per reading taken. The load response and the crack propagation of the specimen were monitored throughout the test.

Table 2. Details of specimen

Specimen	Embedded length of hidden corbel in column, l_c (mm)	Embedded length of corbel in beam, l_b (mm)	SHS hidden corbel A size (mm)	SHS hidden corbel B size (mm)	Grout strength, $f_{u,g}$ (N/mm^2)
RC0	Monolithic reinforced concrete connection				
PC0	Precast concrete connection without SHS hidden corbel				
PC1	125	300	50.8	38.1	40
PC2	125	300	76.2	63.5	40
PC3	125	300	101.6	88.9	40
PC4	75	300	101.6	88.9	40
PC5	175	300	101.6	88.9	40
PC6	125	200	101.6	88.9	40
PC7	125	400	101.6	88.9	40
PC8	125	300	101.6	88.9	20
PC9	125	300	101.6	88.9	NIL

** Thickness of all SHSs was 3 mm*

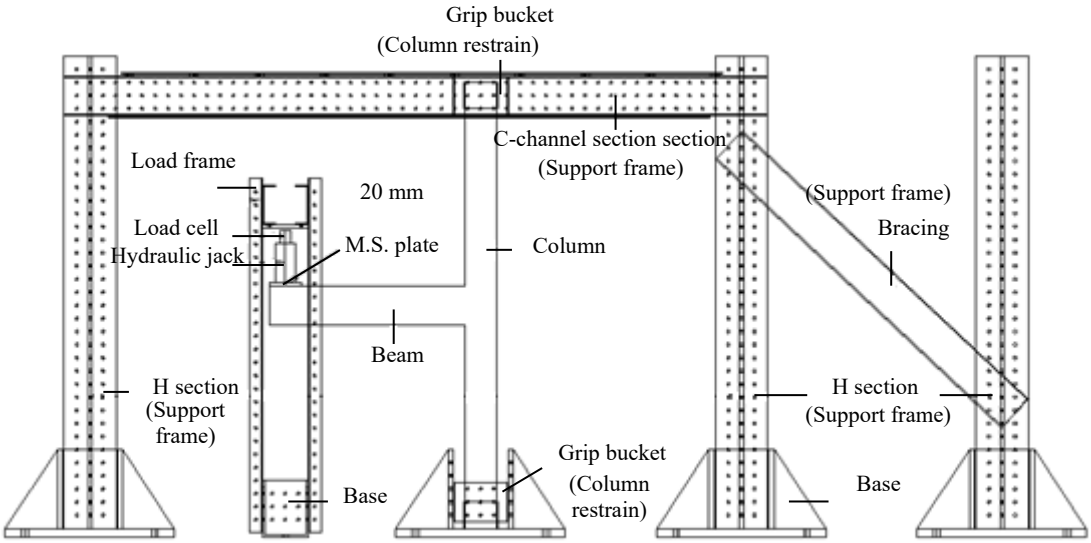

(a) Loading frames

(b) Test setup

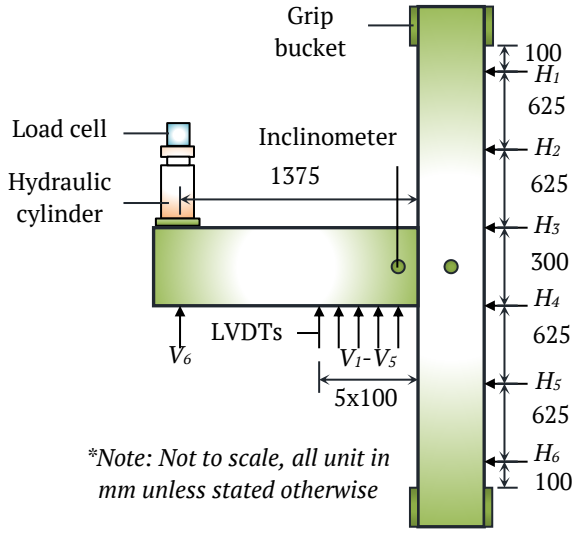

(c) Instrumentation

Figure 5. Test setup and instrumentation

3 RESULTS AND DISCUSSIONS

3.1 Material Properties

The properties of the materials used to fabricate the specimens are shown in Tables 3 and 4. The compressive strength of the concrete and grout were quite consistent. In addition, they were also close to their intended strengths of 40 N/mm^2. The yield strengths of the steel components were all higher than their nominal strengths of 460 N/mm^2 and 250 N/mm^2, respectively. Practically, the quality of materials was considered acceptable.

3.2 Test Results

The results of the specimens are shown in Table 5. The first crack load was determined immediately a crack was detected on the surface of the specimen. The ultimate load had the highest load recorded throughout the test.

The data were further recomputed into the moment-rotation (M-ϕ) response using Equations (1) and (2), as shown in Table 6 and Figure 6.

$$M_i = P_i L \quad (1)$$

where M_i is the moment acting on the connection at different load levels (kNm), P_i is the load acting on the beam (kN), and L is the distance of the point load from the connection face (m).

$$\phi_i = \phi_{b,i} - \phi_{c,i} \quad (2)$$

where $\phi_{b,i}$ and $\phi_{c,i}$ are the moment rotation of the beam and column respectively (milli-rad).

Table 3. Compressive strength of concrete and grout of the specimens

Specimens	Compressive strength of concrete, $f_{c,u}$ (N/mm^2)	Compressive strength of grout, $f_{g,u}$ (N/mm^2)
RC0	36.6	-
PC0	38.0	-
PC1	38.6	40.1
PC2	38.7	40.2
PC3	39.3	40.0
PC4	39.6	40.4
PC5	39.2	39.9
PC6	41.3	40.4
PC7	39.0	39.4
PC8	40.1	20.0
PC9	39.8	-

**Average values of 2 and 3 cube samples for concrete and grout, respectively.*

Table 4. Tensile strength of steel components of the specimens

Specimen	Yield Strength, f_y (N/mm^2)	Ultimate strength, f_u (N/mm^2)	Young Modulus, E (kN/mm^2)	Strain Elongation (%)
Steel bars T16	525	611	210	14.47
Steel bars R8	450	506	234	14.85
20 mm thick steel endplate	303	384	229	19.67
38.1 mm SHS	321	358	202	7.64
50.8 mm SHS	278	338	202	11.99
63.5 mm SHS	319	399	202	9.39
76.2 mm SHS	303	351	204	9.79
88.9 mm SHS	326	375	200	11.63
101.6 mm SHS	346	389	202	9.70

**Average values of 3 steel samples*

Table 5. Test results

Specimen	First Crack				Ultimate state			
	Load, P_{ic} (kN)	Vertical displacement, δ_{ic} (mm)	Beam rotation, $\phi_{b,ic}$ (°)	Column rotation, $\phi_{c,ic}$ (°)	Load, P_u (kN)	Vertical displacement, δ_u (mm)	Beam rotation, $\phi_{b,u}$ (°)	Column rotation, $\phi_{c,u}$ (°)
RC0	7.5	2.0	0.06	0.03	39.1	50.0	1.69	0.44
PC0	8.3	3.1	0.10	0.01	41.3	80.1	2.9	0.27
PC1	8.2	4.1	0.16	0.03	42.4	76.1	2.28	0.36
PC2	10.0	4.4	0.15	0.03	45.7	96.0	2.67	0.39
PC3	9.7	3.7	0.09	0.03	47.3	102.2	2.28	0.58
PC4	5.7	3.6	0.13	0.02	46.3	116.2	3.49	0.48
PC5	6.5	2.0	0.05	0.02	49.5	86.0	1.84	0.43
PC6	9.8	4.0	0.12	0.02	42.1	72.0	1.82	0.25
PC7	10.2	3.8	0.10	0.04	49.8	60.0	1.97	0.85
PC8	10.6	3.8	0.09	0.03	46.8	94.1	2.18	0.57
PC9	8.3	5.9	0.20	0.03	44.7	106.1	3.55	0.43

Table 6. Moment and rotation of the specimen

Specimen	First crack			Ultimate state		
	Moment, M_{ic} (kNm)	Rotation, ϕ_{ic} (10^{-3} rad)	Stiffness, S_{ic} (kNm/10^{-3} rad)	Moment, M_u (kNm)	Rotation, ϕ_u (10^{-3} rad)	Stiffness, S_u (kNm/10^{-3} rad)
Equation	(1)	(2)	(3)	(1)	(2)	(3)
RC0	10.3	0.5	20.6	53.8	21.8	2.5
PC0	11.4	1.6	7.1	56.8	45.9	1.2
PC1	11.3	2.3	4.9	58.3	33.5	1.7
PC2	13.8	2.1	6.6	62.8	39.8	1.6
PC3	13.3	0.9	14.8	65.0	29.7	2.2
PC4	7.8	1.8	4.3	63.7	52.5	1.2
PC5	8.9	0.5	17.8	68.1	24.6	2.8
PC6	13.5	1.6	8.4	57.9	27.5	2.1
PC7	14.0	0.7	20.0	68.5	19.5	3.5
PC8	14.6	1.1	13.3	64.4	28.1	2.3
PC9	11.4	2.8	4.1	61.5	54.5	1.1

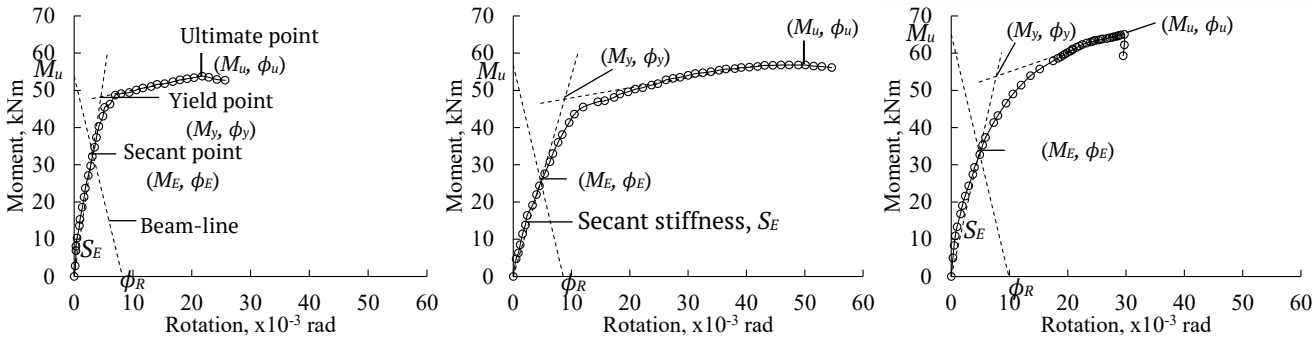

(a) Specimen RC0 (b) Specimen PC0 (c) Specimen PC3

Figure 6. Determining the properties of connection using beam-line method

The beam-line method proposed by Elliott (2002) was used to determine the properties of the specimens. The secant point (M_E, ϕ_E) was determined based on the characteristics of a perfectly rigid and pinned connection. A rigid connection is bound to have a moment capacity equivalent to the fixed-end moment of the beam, as shown in Equation (3). On the contrary, the rotation of a pinned connection is governed by the rotational limit of an RC beam, as shown in Equation (4).

$$M_R = \frac{wL_b^2}{12} \quad (3)$$

$$\phi_R = \frac{wL_b^3}{24EI_b} \quad (4)$$

where M_R is the fixed-end moment of the continuous beam (kNm), ϕ_R is the allowable rotation of an RC beam (milli-rad), w is the uniformly distributed load acting on the beam (kN/m), L_b is the beam span (m), E is the elastic modulus of concrete (kNm/milli-rad), and I_b is the second moment of inertia on the beam cross-section (m^4).

Besides, assuming the ultimate moment capacity of the specimen, M_u was equivalent to the fixed-end moment of the beam, M_R, the allowable rotation of the connection, ϕ_R is as stated in Equation (5).

$$\phi_R = \frac{M_u L_b}{2EI_b} \quad (5)$$

where M_u is the ultimate moment capacity of the connection (kNm), L_b is the effective span of beam (m), assumed to be 6 m (typical beam span), E is the elastic modulus of the beam (kN/m^2), which was obtained as 35 GPa for a grade 40 (BS-EN 1992-1-1:2004) concrete, and I_b is the second moment of inertia on the beam (m^4).

The beam-line intercepted the M-ϕ curve at the secant point (M_E, ϕ_E). The gradient connecting the secant point with the Origin was considered the secant stiffness, S_E (Equation (6)).

$$S_E = \frac{M_E}{\phi_E} \quad (6)$$

The secant stiffness line was further extended to the intercept with a best-fit straight line of the M-ϕ curve at the ultimate state to determine the yield point (P_y, ϕ_y) (Figure 6). The properties of the connection were determined by using the Beam-Line Method, as shown in Table 7.

The first crack moment, M_{ic}, was discovered to be relatively equivalent to 1/5 of the ultimate moment, M_u (refer to the ratio of M_{ic}/M_u reported in Table 8). However, before the first crack, the connection was in its best condition and had the highest degree of stiffness.

The secant moment, M_E was conservatively considered as the designed strength of the connection, M_d (Lim, 2014). This was relatively 2 to 3 times equivalent to the first crack moment, M_{ic} as well as approximately 29% to 61% of the ultimate moment, M_u depending on the secant stiffness (Table 8). In general, the design moments, M_d of the PC connections, were generally lower than their ultimate moments, M_u. This led to a sizeable unutilized connection strength between M_u and M_d. When the M_u and ϕ_R are similar, the unutilized strength of the connection can be reduced by increasing its stiffness, as shown in Figure 7.

Table 7. Test results

	Rotation limit, ϕ_R (10^{-3} Rad)	Secant moment, M_E (kNm)	Secant rotation, ϕ_E (10^{-3} rad)	Secant stiffness, S_E (kNm/10^{-3} rad)	Yield moment, M_y (kNm)	Yield rotation, ϕ_y (10^{-3} rad)
Equation	(5)			(6)		
RC0	8.2	32.9	3.1	10.6	47.8	4.5
PC0	8.6	25.4	4.7	5.4	47.6	8.8
PC1	8.9	23.3	5.4	4.3	51.8	12.0
PC2	9.6	28.2	5.3	5.3	49.0	9.2
PC3	9.9	33.4	4.8	7.0	53.6	7.7
PC4	9.7	18.3	6.9	2.7	42.4	16.0
PC5	10.4	34.7	5.1	6.8	54.4	8.0
PC6	8.8	27.4	4.7	5.8	51.3	8.8
PC7	10.4	35.1	5.0	7.0	55.5	7.9
PC8	9.8	33.5	4.7	7.1	52.0	7.3
PC9	9.4	20.5	6.2	3.3	48.9	14.8

Table 8. Performance ratio

Specimen	M_{ic}/M_E	M_{ic}/M_y	M_{ic}/M_u	M_E/M_u	M_y/M_u	ϕ_E/ϕ_R	ϕ_y/ϕ_R	ϕ_u/ϕ_R	ϕ_u/ϕ_y
RC0	0.31	0.22	0.19	0.61	0.89	0.38	0.55	2.7	4.8
PC0	0.45	0.24	0.20	0.45	0.84	0.55	1.02	5.3	5.2
PC1	0.48	0.22	0.19	0.40	0.89	0.61	1.35	3.8	2.8
PC2	0.49	0.28	0.22	0.45	0.78	0.55	0.96	4.1	4.3
PC3	0.40	0.25	0.20	0.51	0.82	0.48	0.78	3.0	3.9
PC4	0.43	0.18	0.12	0.29	0.67	0.71	1.65	5.4	3.3
PC5	0.26	0.16	0.13	0.51	0.80	0.49	0.77	2.4	3.1
PC6	0.49	0.26	0.23	0.47	0.89	0.53	1.00	3.1	3.1
PC7	0.40	0.25	0.20	0.51	0.81	0.48	0.76	1.9	2.5
PC8	0.44	0.28	0.23	0.52	0.81	0.48	0.74	2.9	3.8
PC9	0.56	0.23	0.19	0.33	0.80	0.66	1.57	5.8	3.7

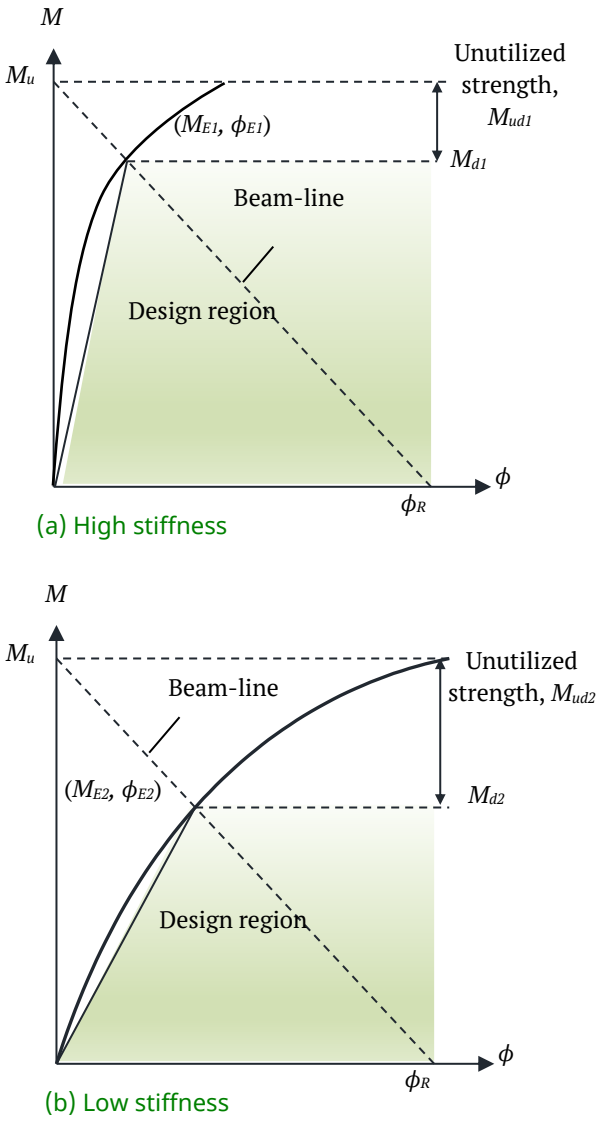

Figure 7. Effect of connection stiffness on the design strength

The yield point was an imaginary state where significant damages to the connection were expected to occur. It was not considered as the design load because (a) it fell above the *M-ϕ* curve, which is not achievable in reality, (b) it underestimated the instantaneous rotation of the connection, realized under the loads, and (c) its rotation occasionally exceeded the rotation limit of the beam ($\phi_y/\phi_R \geqslant 1.0$, as shown in Table 8).

3.3 Classification of Connection

Adopting the principles of Eurocode 3 (BS EN 1993-1-8:2005), a PC connection was classified by its stiffness and strength (Table 9).

Table 9. Classifications of connection based on stiffness and strength

Classification	Stiffness	Requirement
Stiffness (kNm/10^{-3} rad)	Pinned	$S_E \leq \frac{0.5EI_b}{L_b}$
	Semi-rigid	$\frac{0.5EI_b}{L_b} < S_E < \frac{k_bEI_b}{L_b}$
	Rigid	$S_E \geq \frac{k_bEI_b}{L_b}$
Strength (kNm)	Pinned	$M_d \leq 0.25M_{Rd}$
	Partial strength	$0.25M_{Rd} \leq M_d \leq M_{Rd}$
	Full strength	$M_d \geq M_{Rd}$

E is the modulus of elasticity of concrete (kN/m²), I_b is the second moment of inertia (m⁴), L_b is the beam span (m), k_b is equal to 8 and 25 for the braced and unbraced system respectively, M_d is the designed strength of the connection (kNm), M_{Rd} is the moment strength of the members (kNm).

The moment strength of a member, M_{Rd}, was considered to be the smaller value of the column, $M_{Rd,c}$, and the beam, $M_{Rd,b}$ (Equation 7), determined using Equation 8 as the moment strength of an RC member.

$$M_{Rd} = \min(M_{Rd,c}, M_{Rd,b}) \quad (7)$$

$$M = \frac{f_{yk} z A_s}{\gamma_c} \quad (8)$$

where f_{yk} is the specified yield strength of the reinforcement bars, γ_c is the partial factor of safety of steel, A_s is the cross-sectional area of the bar, and z is the lever arm of the stress block diagram (mm), which were all assumed as 500 N/mm², 1.15, 402 mm² for 2T16, and 0.95*d* respectively. In general, the connection was considered to be semi-rigid with partial strength, as shown in Table 10.

Table 10. Classification of the connection by stiffness

Classification	Stiffness					Strength		
Specimen	Pinned (kNm/10^{-3} rad)	Braced frame (kNm/10^{-3} rad)	Unbraced frame (kNm/10^{-3} rad)	Secant stiffness, S_E (kNm/10^{-3} rad)	Class	Design moment, M_d (kNm)	M_d/M_{Rd}	Class
PC0	1.6	26.3	82.0	5.4	S	25.4	0.73	P
PC1	1.6	26.3	82.0	4.3	S	23.3	0.67	P
PC2	1.6	26.3	82.0	5.3	S	28.2	0.81	P
PC3	1.6	26.3	82.0	7.0	S	33.4	0.96	P
PC4	1.6	26.3	82.0	2.7	S	18.3	0.53	P
PC5	1.6	26.3	82.0	6.8	S	34.7	1.00	F
PC6	1.6	26.3	82.0	5.8	S	27.4	0.79	P
PC7	1.6	26.3	82.0	7.0	S	35.1	1.01	F
PC8	1.6	26.3	82.0	7.1	S	33.5	0.97	P
PC9	1.6	26.3	82.0	3.3	S	20.5	0.59	P

*[1]E_b = 35000000 kN/m^2, I_b = 0.000562500000 m^4, L_b = 6 m; [2]Classification: R – Rigid, S – Semi-rigid, P – Pinned; [3]$M_{Rd,b}$ = 40.4 kNm, $M_{Rd,c}$ = 34.7 kNm, M_{Rd} = 34.7 kNm (Equation 7); [4]F – Full-strength ($M_d/M_{Rd} \geqslant 1.0$), P – Partial-strength ($0.25 < M_d/M_{Rd} < 1.0$), Pn – Pinned ($M_d/M_{Rd} \leqslant 0.25$)

3.4 Parametric Response

The PC connection generally possessed a lower degree of stiffness than the RC. This was attributed to (a) the relative movements of the cold joints between the components and (b) the poor bending resistance of the steel endplate, both of which led to a larger instantaneous rotational deformation under the load.

Nevertheless, the PC connection had a higher ultimate moment capacity, M_u, than the RC due to (a) the extensive usage of the steel components and (b) the enhanced SHS hidden corbel. The PC connection without hidden corbel, PC0, had a M_u 5.6% higher than the RC0. Meanwhile, those with hidden corbel (PC1 to PC9) had a M_u of approximately 7.6% to 27.3% higher than the RC0. Additionally, both the steel endplate and hidden corbel offered bending resistance to the connection, as shown in Figure 8.

The ultimate moment, M_u of the connection increased as the embedded lengths of SHS hidden corbel in the column and beam increased. Furthermore, when the embedded length in the column increased from 75 mm to 150 mm, M_u increased to 6.9%. On the contrary, when the one in the beam increased from 200 mm to 300 mm, the M_u increased to 18.3%. The longer the embedded length, the larger the bearing area for the hidden corbel to effectively transfer stresses from the beam to the column.

The grout in the hidden corbel caused an increase in the ultimate moment of the connection. Nevertheless, the connection with 20 N/mm^2 grout in the hidden corbel (PC8) resulted in a higher M_u of 4.7% compared to that without grout (PC9). However, as the grout strength increased from 20 N/mm^2 to 40 N/mm^2, M_u increased by only 0.9% (PC3 and PC8). Therefore, the grout is weak in respect to flexural bending. Its main function was to prevent the SHS hidden corbel from undergoing lateral deformation that affected the bending resistance of the connection.

3.5 Failure Mode

The failure mode of the specimens (Figure 9) is shown in Table 11. Generally, the load vertically displaced the free end of the beam, leading to the rotational deformation of the connection. The first crack occurred at the cold joint between the PC beam and the steel endplate. Afterward, it developed on the beam's upper surface, which is referred to as the flexural crack. In addition, it was later discovered at the compressive region of the

connection and eventually developed into diagonal and peripheral cracks that passed through and by the SHS hidden corbel, respectively (Figure 9). Many specimens endured spalling at the tension region of the beam, while some experienced crushing at the compressive area. The steel endplate bent considerably, which subsequently led to the dislocation of the steel stud welded to it, thereby resulting in the spalling of concrete.

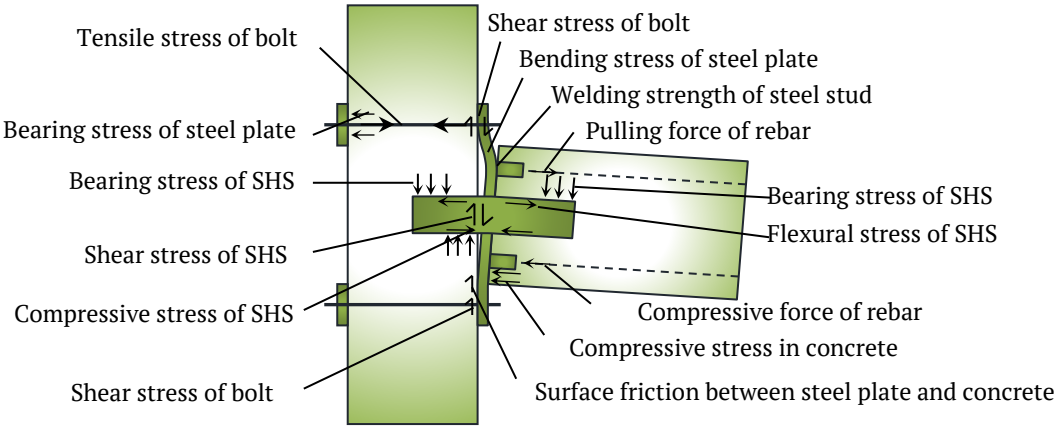

Figure 8. Load resisting mechanism of the connection

Table 11. Failure modes of the specimens

Specimen	Beam				Joint			Column
	Crushing	Spalling	Diagonal crack	Peripheral crack	Flexural crack	Bended endplate	Vertical tearing crack	Diagonal tensile crack
RC0					L		H	L
PC0	H	L			L	H		
PC1	L	H	M			H		L
PC2		M	H			H		
PC3		M	H	M		H		L
PC4	H	H		H		H		L
PC5				H		M		M
PC6	H	M	H			M		M
PC7	H	L		H		M		M
PC8	M	M	H	L		M		H
PC9		H		M		H		L

*Severity rating based on visual observation: H – high, M – moderate, L – Low

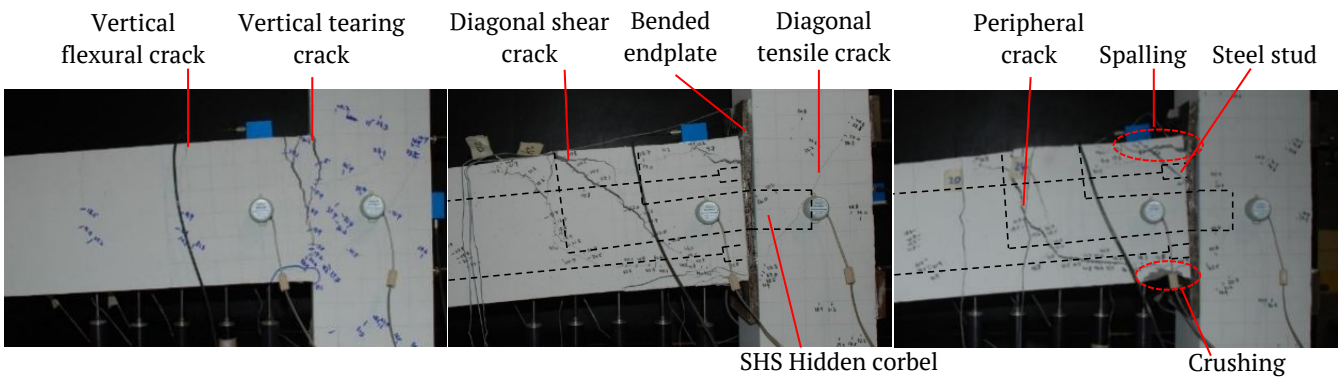

(a) RC0 (b) PC3 (c) PC4

Figure 9. The typical failure mode of the connection

The responses of the connected components under the load are reported as follows (refer to Figure 8)

a) The beam rotation generated bearing stress which acted on the SHS hidden corbel, thereby leading to flexural load.
b) The pulling force of the top reinforcement bar generated bending and tensile stress in the steel endplate and bolts, respectively.
c) The rotational movement of the beam triggered the compressive stress in the bottom reinforcement bars and the concrete. This subsequently led to the frictional resistance between the steel endplate and the concrete.
d) The shear resistance of the bolts and the SHS hidden corbel resisted the vertical load. This further prevented the beam from displacing vertically.

Based on the load resisting mechanism, the capacity of the connection tended to be governed by (a) the tensile strength of the bolt, (b) the bending strength of the endplate, (c) the bending strength of the SHS, (d) the welding strength of the steel stud on the endplate, (e) the pullout strength between the top reinforcement bar and the steel stud and (f) the crushing strength of the concrete at the compressive region, whichever was weaker. In the circumstance that the connection was stronger than the beam and column, the RC member shall govern the load capacity.

The PC connections were generally stronger, as proven by the severe diagonal and peripheral cracks on the beam. Therefore, specimens PC0 to PC9 generally generated a higher ultimate moment, M_u, than the RC0. However, the significant bending deformation of the steel endplate had caused the connection to experience large rotational deformation with poor stiffness. This subsequently led to poor design strength of the connection over the ultimate load. Therefore, to improve the design strength, the effective second moment of inertia of the steel endplate in resisting the bending deformation needs to be increased, as shown in Figure 10.

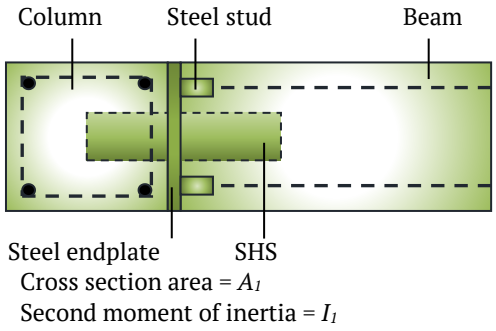

(a) Original design

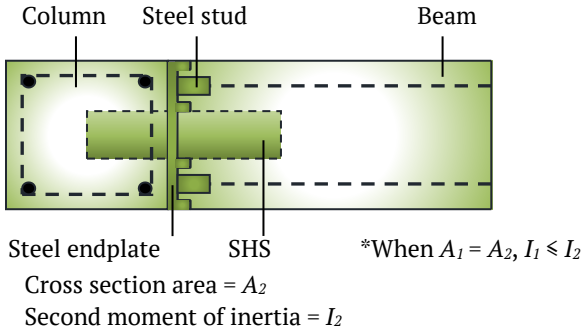

(b) New design

Figure 10. Comparison of the second moment of inertia of the steel endplate

4 FEASIBILITY EVALUATION

The feasibility of the PC connection was evaluated based on the following assessment criteria

a) C1: The moment strength of the PC connection was comparable to the RC. Therefore, both the ultimate strength ratio, $R_{m,u}$, and the design strength ratio, $R_{m,d}$, need to be relatively 1.0.
   i. $R_{m,u} = \frac{M_{u,i}}{M_{u,c}} \geq 1.0$ (9)
   where $M_{u,i}$ and $M_{u,c}$ are the ultimate moment of PC and RC connections respectively (kNm).
   ii. $R_{m,d} = \frac{M_{d,i}}{M_{d,c}} \geq 1.0$ (10)
   Besides $M_{d,i}$ and $M_{d,c}$are the design moment of PC and RC connections respectively (kNm).
b) C2: The connection needs to be ductile for survival purposes. Therefore, the ductility ratio, R_{dc}, has to be approximately 4.0 in the low-moderate seismic regions (Soudki, 1994; Ling et al., 2017).

$$R_{dc} = \frac{\phi_u}{\phi_d} \geq 4.0 \quad (11)$$

where ϕ_u is the rotation of connection at the ultimate state (milli-rad) and ϕ_d is the designed rotation of the connected beam (milli-rad)

c) C3: The connection need not fail earlier than the beam. Therefore, the ultimate rotation of the connection has to be greater than the allowable rotation of the beam, presumably 3 times more.

$$R_r = \frac{\phi_u}{\phi_R} \geq 3.0 \quad (12)$$

d) C4: The design moment should not be too low compared to the ultimate moment in order to ensure that the connection is efficiently utilized. The design ratio, R_d, needs to be relatively 0.5.

$$R_d = \frac{M_d}{M_u} \geq 0.5 \quad (13)$$

where M_d and M_u are the design (kNm), and ultimate moments of the connection (kNm), respectively.

e) C5: In respect to the complexity in predicting the beam rotation, as the SHS hidden corbel of the connection tends to have altered (i.e. shortened) the effective length of the beam in computing ϕ_R, some allowances may be required to ensure the rotation limit is not exceeded. The designed rotation is preferably less than 50% of the allowable rotation.

$$R_a = \frac{\phi_d}{\phi_R} \leq 0.5 \quad (14)$$

where ϕ_d is the design rotation of connection (milli-rad), and ϕ_R is the rotation limit (milli-rad)

The feasibility evaluation of the connection is shown in Table 12. The connections were considered feasible only when all the assessment criteria were fulfilled.

Based on the evaluation, specimen PC3 was discovered to be feasible for PC structure. Irrespective of the fact that it did not have the largest moment capacity, however this specimen performed relatively well in various aspects. The second-best option was the PC8, which had satisfied 5 out of 6 criteria. The non-compliance in criteria C3 (R_r = 2.9) was rather close to the requirement, which is 3.0.

The main difference between specimens PC3 and PC8 was their grout strengths of 40 N/mm^2 and 20 N/mm^2, respectively. This shows the need to have the SHS hidden corbel filled with grout, although this does not necessarily require high strength.

Table 12. Classification of connection by the strength

Criteria	C1(i)	C1(ii)	C2	C3	C4	C5	Score*1	Feasible*2
Ratio	$R_{m,u}$	$R_{m,d}$	R_{dc}	R_r	R_d	R_a		
Equation	(9)	(10)	(11)	(12)	(13)	(14)		
Requirement	⩾1.0	⩾1.0	⩾4.0	⩾3.0	⩾0.5	⩽0.5		
PC0	1.06	0.77	9.8	5.3	0.45	0.55	3/6	N
PC1	1.08	0.71	6.2	3.8	0.40	0.61	3/6	N
PC2	1.17	0.86	7.5	4.1	0.45	0.55	3/6	N
PC3	1.21	1.02	6.2	3.0	0.51	0.48	6/6	Y
PC4	1.18	0.56	7.6	5.4	0.29	0.71	3/6	N
PC5	1.27	1.05	4.8	2.4	0.51	0.49	5/6	N
PC6	1.08	0.83	5.9	3.1	0.47	0.53	3/6	N
PC7	1.27	1.07	3.9	1.9	0.51	0.48	4/6	N
PC8	1.20	1.02	6.0	2.9	0.52	0.48	5/6	N
PC9	1.14	0.62	8.8	5.8	0.33	0.66	3/6	N

*1Score – number of criteria fulfilled / total number of criteria; 2Y – Feasible, N – Not feasible

5 CONCLUSION

In this study, an experimental test was conducted on eleven full-scale T-subframe specimens to investigate the behaviour of precast concrete beam-to-column connection in respect to SHS hidden corbel. The mechanical properties of the connections were determined and classified based on the beam-line method and the Eurocode 3, respectively. The connections were classified semi-rigid and partial strength.

Due to the steel components, the PC connection offered an approximately 6% to 27% higher ultimate moment than the RC. However, due to low stiffness, the design strength of the PC connection was generally lower than the RC.

The SHS hidden corbel contributed to the moment resistance of the connection. Its embedded length in the column and the beam increased the moment strength of the connection. The grout infill was discovered to strengthen the hidden corbel, although the increasing strength of the connection was minimal.

Furthermore, excessive bending deformation of the steel endplate was identified to be the root cause of the low stiffness and design strength of the connection, which subsequently led to the ineffective utilization of the moment capacity. The steel endplate may be modified to increase the second moment of inertia for higher efficiency of the connection design.

The feasibility of the connection was evaluated in various aspects, namely the strength, ductility, serviceability, and design tolerance. The evaluation was carried out based on relative comparison among the test specimens. In addition, specimen PC3 was discovered to fulfill all the evaluation criteria and was therefore considered feasible.

DISCLAIMER

The authors declare no conflict of interest.

AVAILABILITY OF DATA AND MATERIALS

All data are available from the author.

ACKNOWLEDGMENTS

The authors are grateful to the Ministry of Higher Education, Vot 78013, for the Research Grants provided to carry out this research.

REFERENCES

BS-EN 1992-1-1:2004, 2004. Eurocode 2: Design of concrete structures - Part 1-1: General rules and rules for buildings.

BS EN 1993-1-8:2005, 2005. Eurocode 3: Design of steel structures - Part 1-8: Design of joints.

Choi, H. K., Choi, Y. C. & Choi, C. S., 2013. Development and Testing of Precast Concrete Beam-to-Column Connections. *Engineering Structures*, 56, pp 1820-1835.

Elliott, K. S., 2002. *Precast Concrete Structure*, Boston: Butterworth-Heinemann.

Jaspart, J. P., 1996. *Structural Connections: Experimental as Design Tool*. Seminar Structural Assessment: The Role of Large and Full Scale Testing. City University, London

Lim, J. H., 2014. *Experimental Behaviour of Exterior Hybrid Precast Concrete Beam-to-Column Connections Subjected to Monotonic Load*. PhD Thesis, Universiti Teknologi Malaysia.

Lin, F. & Zhao, P., 2020. Behavior of Grouted Sleeve Splice for Steel Profile under Tensile Loadings. *Materials*, 13(9), 2037.

Ling, J. H., Abd. Rahman, A. B., Ibrahim, I. S. & Abdul Hamid, Z. 2017. An Experimental Study of Welded Bar Sleeve Wall Panel Connection under Tensile, Shear, and Flexural Loads. *International Journal of Concrete Structures and Materials*, 11, pp 525-540.

Lu, Z., Huang, J., Li, Y., Dai, S., Peng, Z., Liu, X. & Zhang, M., 2019. Mechanical Behaviour of Grouted Sleeve Splice under Uniaxial Tensile Loading. *Engineering Structures*, 186, pp 421-435.

Soudki, K. A., 1994. *Behaviour of Horizontal Connections for Precast Concrete Load-bearing Shear Wall Panels Subjected to reversed Cyclic Deformations*. PhD thesis, University of Manitoba.

Zheng, Y., Guo, Z., Guan, D. & Zhang, X., 2018. Parametric Study on a Novel Grouted Rolling Pipe Splice for Precast Concrete Construction. *Construction and Building Materials*, 166, pp 452-463.

[This page is intentionally left blank]